Improvement of Silicone Endothelialization by Treatment with Allylamine and/or Acrylic Acid Low-Pressure Plasma

Sophie Monge,[1] André Mas,[1] Amina Hamzaoui,[1,2] Camille M. Kassis,[3] Joseph M. Desimone,[3] François Schué[1]

[1]*Organisation Moléculaire, Evolution et Matériaux Fluorés (Laboratoire de Chimie Macromoléculaire), UMR 5073 CNRS, Université Montpellier II, Place E. Bataillon, 34095 Montpellier Cedex 5, France*
[2]*Biomedical Engineering Laboratory, Florida International University, University Park Campus, Miami, Florida 33199*
[3]*Department of Chemistry CB #3290 Venable and Kenan Laboratories, University of North Carolina at Chapel Hill, Chapel Hill, North Carolina 27599-3290*

Received 26 September 2001; accepted 3 May 2002

ABSTRACT: Plasma polymerization of allylamine, acrylic acid, and an allylamine/acrylic acid mixture on Silastic® silicone rubber led to a strong increase in the silicone rubber's hydrophilicity and surface energy. Analysis of the deposited layer by X-ray photoelectron spectroscopy with 20° and 70° takeoff angles showed segregation of the atoms according to the depth and the incorporation of amino groups, oxygenated groups, and both. The endothelialization of untreated and treated samples was evaluated by the seeding and growth of aorta epithelial cells from pigs in cellular adherence (%), doubling time (in hours), and confluent density (10^4 cells/cm^2). The best results were obtained with the allylamine/acrylic acid mixture treatment, which brought a biocompatibility to Silastic® similar to classic tissue culture on polystyrene plates. The interpretation was based on the presence of NH_3^+/CO_{2-} microareas in the deposited layer. © 2003 Wiley Periodicals, Inc. J Appl Polym Sci 87: 1794–1802, 2003

Key words: plasma treatment; silicone biocompatiblity

INTRODUCTION

The development of various materials has led to important applications in the field of medicine and surgery. Nevertheless, two essential points must be considered: (1) biocompatibility—the material must not create toxic or allergic reactions in a biological environment—and (2) structural properties—the material must resist compression and tension and have good flexibility.[1]

Although the biocompatibility of biomaterials has improved over the years, a perfect surface has not yet been found, and the synthesis of biomaterials having both good biocompatibility and good structural properties is not easy.

The endothelium represents the ideal biocompatible surface. In an attempt to overcome the toxic nature of artificial materials, the technique of seeding the surface of biomaterials with endothelial cells has been developed over the last two decades. When appropriate polymers have been used, the endothelial seeding has been shown to promote the rapid growth of an endothelial lining. A major problem with the seeding procedure is that most currently used materials are resistant to endothelial cell attachment and therefore must be precoated with protein or adhesive substrates (such as fibronectin, fibrin, and collagens) to render the surface more favorable to endothelial cell attachment. Unfortunately, the ideal adhesive substrate remains to be established: synthetic materials and prostheses do not develop in every case in an endothelial lining after a long implantation in living tissues. To achieve endothelialization, modifications of surfaces that are more sophisticated than simple protein applications needs to be performed. It seems that the failure of endothelialization is due in large part to an intrinsic material deficiency in the ability of the synthetic surfaces to optimally support the attachment and growth of the seeded cells. These two biological phenomena that make up endothelization—attachment and growth—are different. Cell attachment happens during the first 2 hafter seeding. This initial attachment can be nonspecific and takes place on a range of polymer supports without necessarily leading to cell lining and growth.

It has generally been shown that a hydrophobic surface limits the endothelialization process, whereas a hydrophilic one markedly favors it.[2,3] The nature of the functional groups grafted on the surface is of the utmost importance for the behavior of the cells. Until now, the most appropriate functional groups have not been clearly defined: sulfonic acid,[4] carboxyl acid,[5,6] amino,[7] and hydroxyl[8] groups are often cited. So the polystyrene widely used in tissue culture (marketed as TCPS and Primaria™) has oxygenated and nitroge-

Correspondence to: A. Mas (mas@univ-montp2.fr).

Journal of Applied Polymer Science, Vol. 87, 1794–1802 (2003)

nated functional groups deliberately introduced on the surface in order to successfully improve the endothelialization .[5,9] For that reason surface treatments are being widely developed—to enhance the biocompatibility of numerous polymer materials.

The purpose of the work presented here was to modify the surface chemistry of polymeric biomaterial using a polymerization technology called plasma treatment[10–12] or radio frequency glow discharge (RFGD). This technique provides a unique and powerful method for changing surface properties by depositing a plasma layer while keeping the bulk structure of the treated material unchanged. Silicone elastomers[13] have already been used in such biomedical applications as catheters and contact lenses and more generally in the cardiopulmonary bypass,[14] in the development of an artificial cornea,[15] and in voice protheses.[16] They have been used in plasma treatment,[17–19] mainly in the field of membrane techniques. But only a few investigations have been pursued in the field of endothelialization.

For all these reasons, we have been interested in the treatment of Silastic®-marketed silicone rubber by plasma polymerization of allylamine, acrylic acid, and a mixture of allylamine and acrylic acid in order to bring nitrogen, oxygen, and both nitrogen and oxygen onto the Silastic® surface. The application of oxygen, nitrogen, or even air plasma to hydrophobic silicon rubber surfaces already have resulted in a strong hydrophilization because of the oxidation of the alkyl groups. However, in this study allylamine and acrylic acid plasma–polymerized monomers were chosen because they might bring many more carboxyl and amino groups than a simple gas; moreover, a deposited layer can cover and completely isolate the treated material from the living environment. The wettability and surface energy, the atomic percentage of the elements, and the nature of the chemical groups of the deposited layer were determined using contact-angle analysis, X-ray photoelectron spectroscopy (XPS), and FTIR–ATR techniques respectively. Then the adhesion and growth of endothelial cells from pigs were evaluated on untreated and treated samples. Finally, we tried to deduce information about the relationship between the characteristics of the plasma-treated Silastic® surface and the ability to promote the endothelialization, which is similar to biocompatibility.

EXPERIMENTAL

Plasma treatment

The details and scheme of the experimental setup used for the plasma treatment were given previously.[20] The reactor contained a pair of parallel aluminum electrodes (12 cm in diameter, 3 cm apart) coupled with an rf generator (13.56 MHz). Silastic® samples were supplied by the Dow Corning Corporation (Midland, MI). Dried samples were placed on the bottom electrode. A vacuum was established at 3 Pa, and the allylamine (Merck) and acrylic acid (Merck) vapor flows were monitored with a Pirani gauge and were regulated to obtain the desired pressure. The rf power was turned on, and the plasma treatment was performed. To complete the treatment, the rf power was turned off and the vapors flows pursued for an additional 10 min. Then the system was pumped down to 3 Pa for 20 min before the reactor was opened.

Contact-angle analysis

Static contact angles with water and diiodomethane were measured with a Kruss G1 goniometer 5 s after the drop was deposited to avoid evaporation or absorption by the substrate. Ten measurements on different surface locations were averaged for each sample. The error of measurement was $\pm 1°$. Surface energy (γ_s) and polar (γ_s^p) and dispersive (γ_s^d) components were calculated with the Owens method. The accuracy was about ± 1 mN/m.

Electron spectroscopy for chemical analysis

Electron spectroscopy for chemical analysis (ESCA) was done via X-ray photoelectron spectroscopy (XPS) using a Perkin-Elmer Physical Electronics Model 5400 spectrometer equipped with a hemispherical capacitor analyzer. The Mg-K_α X-ray source (nonmonochromatic) used to irradiate the samples operates at 15 keV and 400 W. The resolution for the main Mg peak (3d 5/2) at a pass energy of 35.37 eV using this source is 1.04 eV. The background observed is Bremsstrahlung radiation because of electrons that have experienced elastic energy losses emerging from the sample. A Shirley function is used to correct for the background of all spectra. Each analysis was performed with two or three spots per sample, and spectra were acquired about 15–30 days after the plasma treatment with two XPS takeoff angles, 20° and 70°, which were, respectively, 2–3 and 5–7 nm deep. All the standard deviations of the atomic percentages were in the range of 0.3%–0.5%. All binding energies were charge referenced to O_{1s} at 532 eV. The interpretation of bonding energies was based on the results tables.[21,22]

Scanning electron microscopy

Scanning electron microscopy (SEM) analysis of the treated surfaces was used to estimate the texture image and to measure the thickness of the deposited layer by observing slice views (not shown) because it is impossible to remove it by a mechanical gesture. SEM analysis was performed with a Jeol 6300 F instrument.

Infrared spectroscopy (attenuated total reflectance)

The spectra from infrared spectroscopy [attenuated total reflectance (ATR)] spectra were recorded with a Brucker IFS 25 spectrophotometer equipped with a KRS5 crystal (1 × 2.5 cm).

Culture and biological assay with porcine aortic endothelial cells

Seeding chambers

Disk-shaped pieces of Silastic® were sterilized with ethylene oxide and dispatched for the application of the plasma surface treatment operation. The plasma-treated and -untreated control disks were placed into tissue culture polystyrene 24-well plates (Fisher Scientific) and retained with press-fit Teflon outer rings. In this manner a disk of the material was immobilized for a cell culture and cell assay. The culture surface area was 1.1 cm,^{2} and the volume was 1 mL.

Seeding of endothelial cells

Endothelial cells from porcine thoracic aorta[23] grown to confluence in Petri dishes were seeded into the chambers. The cells were left to adhere to the surface material in 800 μL of culture medium. After 2 h the medium was removed, and any nonadhered cells were washed away with fresh medium. The medium was changed every 2 days until the cells were confluent.

Determination of adhesion and growth of endothelial cells

The cells were seeded at a density of 2×10^4 cell/cm^2. Cells counts were taken 2 h after seeding for the determination of cell adhesion and every day thereafter for cell density. The proliferative capacity of the cells was checked in parallel assay on fibronectin-coated tissue culture polystyrene well plates and non-coated tissue culture polystyrene plates. At each experimental time point a culture plate was washed with phosphate buffered saline (PBS; Gibco) and the cells detached with 1% trypsin-EDTA. A Neubauer counting chamber (Hausser Scientific, Pittsburgh, PA) with an aliquot of the suspension was used to count for cells. For ease of cell recognition all aliquots used for counting were diluted at a 1:3 ratio with crystal violet (0.1%) in citric acid (0.1 mol/L).

The morphology and number of adhered cells were also evaluated by microscopic examination. For this purpose cells were fixed in 3.7% formalin (Sigma Chemicals, St. Louis, MO) for 20 min and stained with May-Grunwald Giemsa (Sigma). The cells were examined and counted under a inverted-phase contrast microscope (Olympus, CK2).

TABLE I
Binding Energies (eV) and Atomic Percentages of Element (at %) of Untreated Silastic® with Two Analyses Takeoff Angles

	Binding energy (eV)		Atomic percentage (%)	
Element	20°	70°	20°	70°
C_{1s}	284.8	284.6	43.7	42.7
O_{1s}	532	532		
	533.6	533.5	32.5	34.2
Si_{2p}	101.6	101.5		
	102.6	102.7	23.8	23.1

RESULTS AND DISCUSSION

First measurements were done on untreated Silastic®. The contact angles were 101° with water and 65° with diiodomethane. These values provided evidence of an important characteristic of the Silastic® surface, its hydrophobicity, as the surface energy calculated by the Owens method was 25.8 mN/m.

XPS analysis of the reference sample (untreated Silastic®) showed the presence of carbon, oxygen, and silicon (Table I). Based on the curve fits showed, two types of oxygen and two types of silicon were present. The lower-binding energy O component was most likely the Si—O species, whereas the higher-binding energy species could be SiO_2. The lower-binding energy Si_{2p} species is likely a result of Si—O (as in polydimethylsiloxane), whereas the higher-binding energy component could be a result of Si with at least one additional oxygen present (as SiO_2). The C:Si ratio in the untreated Silastic® structure was 1.85.

Allylamine plasma treatment

Plasma polymerization of allylamine was achieved at a power of 75 W under a pressure of 40 Pa. Two successive 30-min treatments were done to produce a homogeneous film. These treatments considerably improved the surface hydrophilicity (Table II), leading to widely higher surface energies; however, these values evolved with time (Fig. 1).

Moreover, in XPS analysis modifications of the material could be observed (Table III). First, the overall atomic percentages apparently showed little change for C_{1s} and O_{1s}. At 70— there was a decrease in the Si_{2p} atomic percentage, compared with both the 20° data and the reference sample. This may suggest surface segregation of the silicon species from the plasma treatment. In addition, a nitrogen signal at both angles, but larger at 7°, was found to be present. In examining the individual species, it appeared that both individual oxygen and silicon components had not changed dramatically. There was a slight decrease in the atomic percentage of the lower-binding energy component of Si_{2p} at 20° and a more marked decrease

TABLE II
Evolution of Contact Angle of Plasma-Treated Silastic® with Storage Time in Days (Day 1 Means Just after Plasma Treatment)

Plasma treatment	θ_{H_2O} (°)			θ_{12CH_2} (°)		
	day 1	day 15	day 30	day 1	day 15	day 30
Untreated Silastic®	101			65		
Allylamine	66	93	97	56	60	64
Acrylic acid	44	88	94	39	75	93
Allylamine/acrylic acid	67	88	90	45	54	58

at 70°, possibly a result of the surface segregation. However, we noticed an important changes in the C_{1s} region. Two new higher-binding energy components arose in the 70° spectrum, at approximately 286.2 and 288.3 eV. It was speculated that the 286.2 component might be a result of either C—O or C—N because nitrogen was present on the surface, whereas the 288.3 eV component might correspond to a carbonyl-type species.

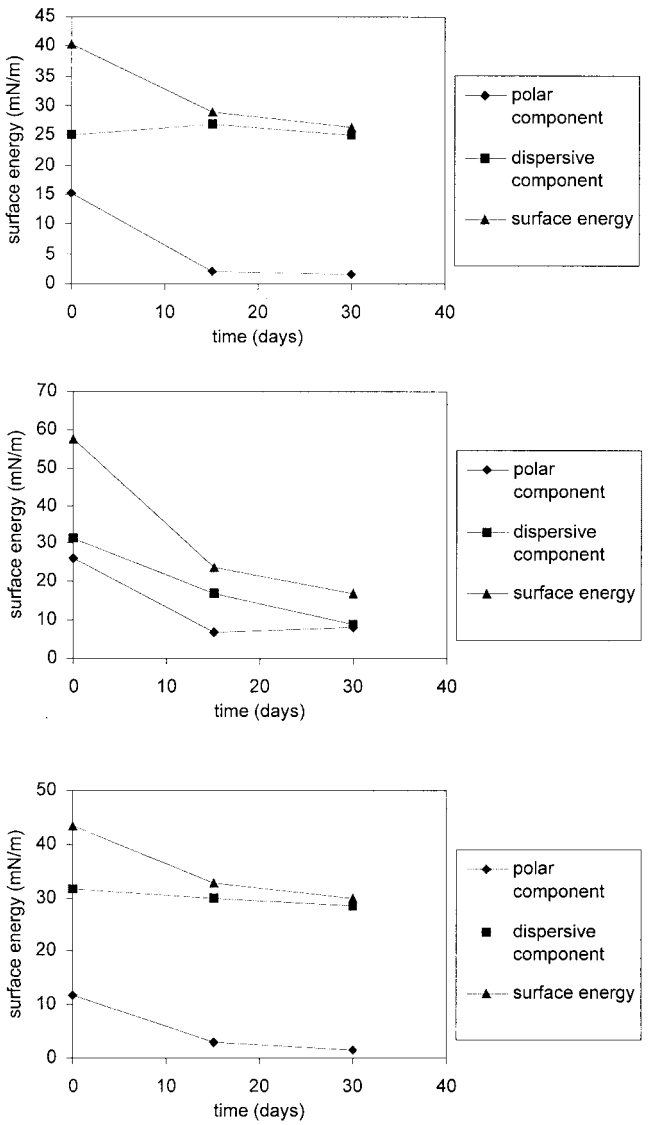

Figure 1 Surface energies (mN/m) of Silastic® treated by (a) allylamine plasma, (b) acrylic acid plasma, and (c) allylamine/acrylic acid mixture plasma.

The ESCA results were confirmed by FTIR–ATR spectroscopy, which showed a probable $\nu_{C=N}$ band at 1660 cm^{-1} and a ν_{NH} band at 3290 cm^{-1}. For this, dry samples were used to avoid the most water absorption. These two bands did not exist in the untreated Silastic® (Fig. 2). We can reasonably suggest that imine and amide groups are present on the surface.

Finally, scanning electron microscopy showed a smooth, homogeneous, and thick film, with a depth approximately equal to 300 nm (Fig. 3).

Acrylic acid plasma treatment

Optimized plasma polymerization of acrylic acid (100 W, 30 Pa, 2 successive 30-min durations) led to a film on the Silastic® surface that was more hydrophilic than that obtained using allylamine. The contact angles were lower (Table II), and as a consequence the surface tension was higher (Fig. 1).

XPS analysis (Table IV) showed that the modifications observed were quite similar to those of the material treated with plasma of allylamine. The overall atomic percentages showed little change in the overall C_{1s} and O_{1s} atomic percentages. At 70° there seemed to be a decrease in the Si_{2p} atomic percentage, compared with both the 20° data and the reference sample, also probably a result of the surface segregation of the

TABLE III
Binding Energies (eV) and Atomic Percentages of Elements (at %) of Silastic® Treated by Allylamine Plasma with Two Analyses Takeoff Angles

Element	Binding energy (eV)		Atomic percentage (%)	
	20°	70°	20°	70°
C_{1s}	284.9	284.7		
		286.2	43.3	45.3
		288.3		
O_{1s}	532	532		
	533.6	533.5	32.8	32.9
Si_{2p}	101.9	101.7		
	103.1	102.9	22.9	18.1
N_{1s}	400.1	399.8	1.0	3.7

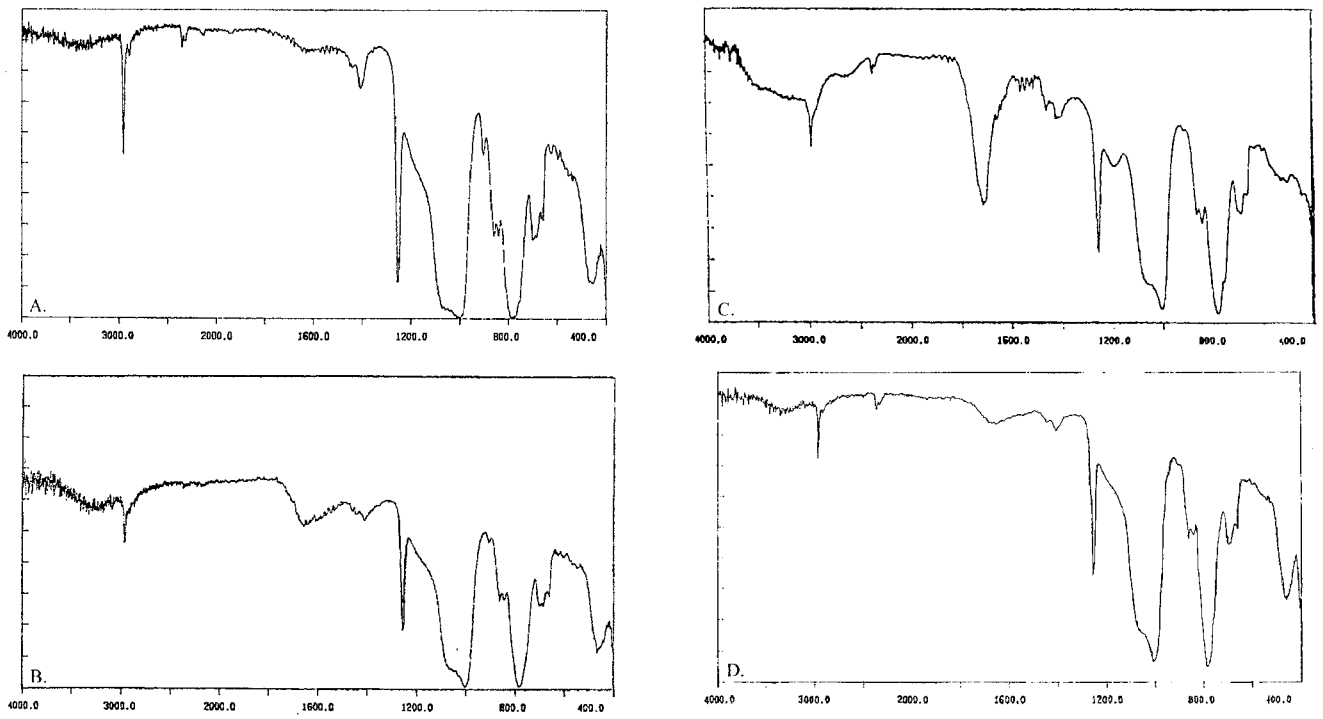

Figure 2 FTIR–ATR spectra of (a) Silastic®, (b) allylamine, (c) acrylic acid, and (d) allylamine/acrylic acid mixture plasma–treated Silastic®.

silicon species. In examining the individual species, we noticed that both oxygen and silicon components had changed slightly. On the other hand, changes occurred in the C_{1s} region. Two new higher-binding energy components had arisen in the 70° spectrum, at approximately 286.3 and 288.5 eV, which might correspond to, respectively, the C—O species and a carbonyl type species.

Furthermore, the existence of C═O groups was confirmed by FTIR/ATR, with the $\nu_{C=O}$ band at 1705 cm^{-1}, which could belong to a ketone, acid, or ester group. We also noticed the ν_{OH} band up to 3000 cm^{-1} (Fig. 2) and probably the carboxyl group were present on the surface.

Scanning electron microscopy showed a smooth and slightly cracked film, thinner than that of allylamine plasma, about 200 nm deep (Fig. 3).

Plasma treatment of an allylamine and acrylic acid mixture

A plasma treatment of Silastic® with a mixture of the two monomers was done to introduce functional groups from allylamine (C═N, NH) and acrylic acid (C═O, OH) on the surface. Some previous experiments led us to select the following treatment parameters, which provided a stable discharge, easy control of the treatment and the best wettability of the treated supports.

Radio frequency glow discharge was first performed with acrylic acid (50 W, 30 Pa, 10 min) followed by a treatment with allylamine (35 W, 40 Pa, 10 min). Then mixture plasma polymerization was achieved (power: 35 W; mixture: acrylic acid 20 Pa completed to 40 Pa with allylamine; treatment duration: 10 min). Plasma polymerization of both allylamine and acrylic acid permitted a great improvement of the surface hydrophilicity. The contact angles showed the wettability improvement on day 1 (Table II). The values were not stable with storage time but remained smaller than those determined with allylamine or acrylic acid separate plasmas. After 30 days the surface energy was equal to 30 mN/m (Fig. 1) compared with 26 mN/m and 17 mN/m for, respectively, the allylamine and acrylic acid plasmas.

The main characteristic that XPS analysis showed was the presence of a large nitrogen signal, which was bulk-segregated, whereas the silicon was surface- segregated. The nitrogen atomic percentages were 4.4 (α = 20°) and 10.8 (α = 70°). These values (Table V) were higher than those for the plasma of each monomer. There appears to have been an increase in the overall carbon signal and conversely a decrease in the total oxygen signal compared with the reference sample. We also noticed an increase in the 286 eV component, particularly at 70°. Furthermore, there was an apparent decrease in the higher-binding energy oxygen component, again particularly at 70°.

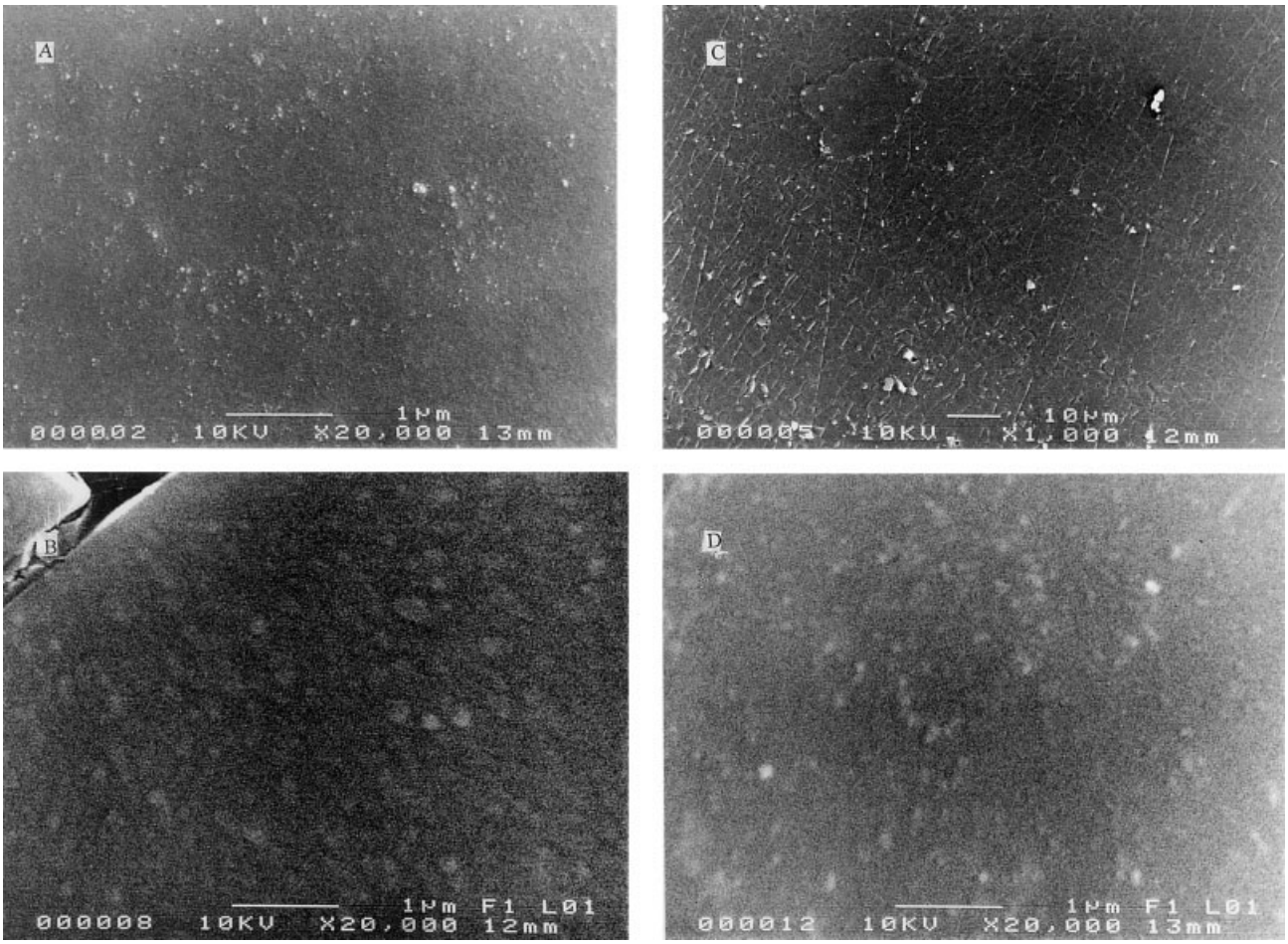

Figure 3 Scanning electron micrographs of (a) Silastic®, (b) allylamine, (c) acrylic acid, and (d) allylamine/acrylic acid mixture plasma–treated Silastic®.

Consequently, we concluded that the mixture plasma allowed the more important incorporation of functional groups that were otherwise brought to the fore with FTIR–ATR spectroscopy. Indeed, we noticed $\nu_{C=N}$ at 1660 cm^{-1} and ν_{OH} or ν_{NH} at 3390 cm^{-1} (Fig. 2) with weak absorption because of the thinness of the layer.

Finally, at the structural level, scanning electron microscopy showed a very slightly cracked film with a depth of 40 nm (Fig. 3).

The three kinds of plasma polymerizations permitted a great improvement of the surface hydrophilicity by the incorporation of functional groups onto the

TABLE IV
Binding Energies (eV) and Atomic Percentages of Elements (at %) of Silastic® Treated by Acrylic Acid Plasma with Two Analyses of Takeoff Angles

	Binding energy (eV)		Atomic percentage (%)	
Element	20°	70°	20°	70°
C_{1s}	284.7	284.8		
		286.3	43.0	45.1
		288.5		
O_{1s}	532	532		
	533.6	533.5	33.9	37.8
Si_{2p}	101.9	101.7		
	103.2	103.0	23.1	17.1

TABLE V
Binding Energies (eV) and Atomic Percentages of Element (at %) of Silastic® Treated by Allylamine and Acrylic Acid Mixture Plasma

	Binding energy (eV)		Atomic percentage (%)	
Element	20°	70°	20°	70°
C_{1s}	284.9	284.9		
	286.7	286.6	48.5	53.2
	288.4	288.3		
O_{1s}	532	532		
	533.6	533.6	30.5	28.2
Si_{2p}	101.8	101.7		
	103.1	102.8	16.6	7.8
N_{1s}	400.3	400.1	4.4	10.8

surface, notably acid groups, amide groups, or both. This was confirmed by ESCA measurements, which were done about 15–30 days after the treatment. Nevertheless, in the three cases hydrophilicity decreased according to the storage time. For all plasmas the silicon atomic percentage was greater in the depths (4–6 nm) than on the surface. Actually, movements of macromolecular chains might occur on the surface of the film, leading to a reorientation of polar groups toward the material bulk to minimize the interfacial energy. This phenomenon was favored by the high flexibility of silicone as well as an inadequate crosslinking of the plasma layer itself because of an inconvenient appropriateness between the power and the gas flow during the plasma treatment. We also considered the migration of short macromolecular chains containing silicon toward the surface. This interpretation was confirmed by various authors for high wettability films.[24–26] Thus, the surface of polymers should not be seen as a rigid plane but as reorganizing according to the environment.[27] Basically, putting the samples in water permitted the attainment of back hydrophilicity improvement. Thus, cells seeding at the film surface led to the restoring of properties observed just at the end of treatment. For the mixture plasma the carbon and nitrogen amounts were higher on the surface than were those of the allylamine or acrylic acid plasmas. Chain movements were then less important for the mixture, which showed there was a higher crosslinking on the surface. The significant C:Si ratio was probably a result of an important mixing and the incorporating of the two monomers.

Scanning electron microscopy showed a thin plasma layer. Consequently, this film was more compact, cohesive, and dense, and it contained more functional groups than those obtained by the allylamine or acrylic acid plasmas.

The functional groups' incorporation mechanisms are very complex and difficult to demonstrate. Nevertheless it is well known that plasma mechanisms are based on reactions of radicals from monomers and the surface.

The results described above allow for some explanations. For allylamine plasma the polymerization was done with allylamine bonds breaking and recombining. So there was no preference between imine or amide entities. A possible mechanism for allylamine plasma, where P indicates the macromolecular chain, is suggested below. The plasma polymerization of allylamine might proceed in this way despite the stabilization of the radical if the very particular reactions taking place in the plasma state are considered. In our study amide formation was a result of oxygen incorporation into the plasma film.[28–30] It was a product of interactions between radicals remaining in the plasma-deposited polymers and oxygen from the air when the material was taken out of the reaction vessel. The proposed mechanism is consistent with FTIR–ATR results, which showed C═N and NH groups, whereas ESCA showed the existence of carbonyl-type species.

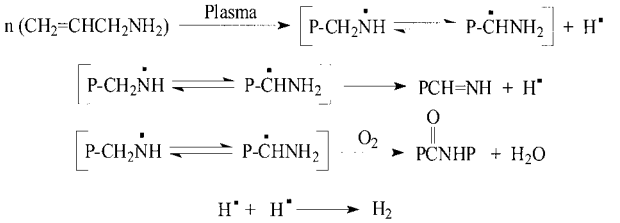

Concerning acrylic acid plasma, a reaction mechanism similar to radical chain polymerization is often put forward. It can be written as:

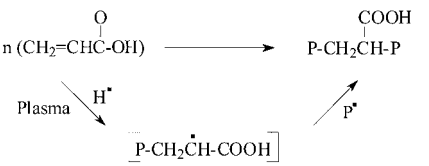

For allylamine and acrylic acid plasma the coexistence of the precedent mechanisms described is probable.

Endothelialization of samples

The treated samples were submitted to a biological assay using endothelial cells (EC) from porcine aortas. Tests were done on untreated Silastic® as well as Silastic® treated with allylamine or/and acrylic acid low-pressure plasma. The proliferative capacity of the cells was checked in parallel assay on noncoated tissue culture polystyrene plates (PS) and on fibronectin-coated tissue culture polystyrene (PS/Fn) well plates. PS and PS/Fn were references that were biocompatible and on which growth cell was important. Both cellular adherence and cellular growth were examined. A surface allowing cell adhesion was not necessary for leading to growth.

In our study all the treatments developed (allylamine and/or acrylic acid plasma) permitted endothelial cell adherence and growth (Fig. 4 and Table VI), although no adhesion was observed on untreated Silastic®. The percentage of seeded cells was close to the polystyrene value and weaker than the fibronectin-coated polystyrene value.

The EC on Silastic® treated by acrylic acid had a slower cellular growth (Fig. 5). Moreover, the doubling time—time necessary for a cell to divide—was significantly higher (39.9 h) than for the references (28.9 h), whereas the doubling time for allylamine (33.5 h) and the mixture (30.7 h) plasma were only slightly different from the references. Finally, the EC confluent density on Silastic® treated by acrylic acid

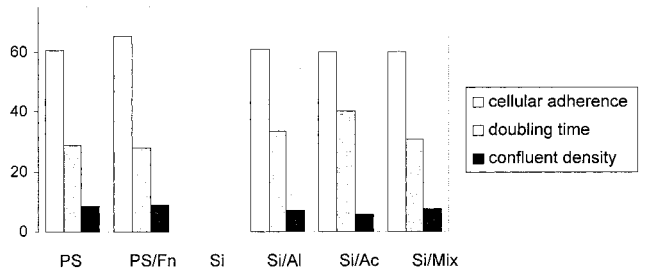

Figure 4 Cellular adherence (% of seeded cells), doubling time (h), and confluent density (10^4 cells/cm^2) for polystyrene (PS), fibronectin-coated polystyrene (PS/Fn), untreated Silastic® (Si), Silastic®-treated by allylamine plasma (Si/Al), acrylic acid plasma (Si/Ac), and allylamine/acrylic acid mixture plasma (Si/Mix).

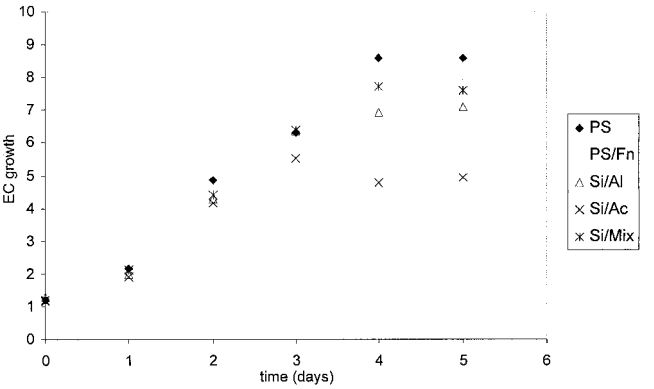

Figure 5 Endothelial cell growth with function of time for Silastic® treated by different plasmas (see Fig. 4 for caption).

was clearly lower than that of the references and both the allylamine and mixture plasmas.

In conclusion, the best biological results (Table VI) were obtained with the mixture and allylamine plasmas. In fact, the biocompatibility improvement was a result of the introduction of polar groups on the surface of the Silastic®. Even if the surface wettability had arisen in the adherence and growth processes, surface chemistry (or charge surface) resulting from the charged functional groups at the physiological pH was a very important factor in the cell adherence, spreading, and growth phenomena.

We have shown that allylamine plasma allowed EC adherence and growth. The amino groups of the Silastic® surface were probably positively charged in the culture environment (pH 7.3–7.4). As most cells and serum proteins were negatively charged on their surface, electrostatic interactions between protein surfaces and positively charged amino groups could occur.

The carbonyl groups brought by acrylic acid plasma were probably negatively charged (pKa slightly up, to 10) in the culture environment (pH 7.3–7.4), forbidding electrostatic interactions with most of the serum proteins, also negatively charged on their surface.

TABLE VI
Summary Table of Biological Results (see Fig. 4 for caption). Data Represent Mean Values ± Standard Deviations of 13 Independent Experiments Using Aortic Cells from Pigs in Which All Conditions Were Assayed Simultaneously

Material	Cellular adherence (%)	Doubling time (h)	Confluent density (10^4 cells/cm^2)
PS	60.2 ± 9.3	28.9 ± 3.5	8.46 ± 0.92
PS/Fn	65.3 ± 6.5	27.6 ± 3.1	8.74 ± 0.42
Si	no adhesion	no growth	no growth
Si/Al	60.7 ± 5.9	33.5 ± 5	7.23 ± 0.77
Si/Ac	60 ± 5	39.9 ± 6.7	5.66 ± 0.96
Si/Mix	60 ± 4.4	30.7 ± 3.7	7.75 ± 1.06

Then cell adherence of Silastic® treated with acrylic acid resulted from high surface wettability.[15]

For the mixture plasma an interaction between NH_2 and CO_2H groups was considered, which would lead to the formation of NH_3^+/CO_2^- microareas that would improve biocompatibility.[31]

$$\mathrm{PmNH_2 + PnCO_2H \rightarrow PmNH_3^+\ {}^-O\overset{\overset{\mathrm{O}}{\|}}{C}Pn}$$

This interaction would take place in plasma phases on nondeposited oligomers or would exist for the deposited film for close amino and acid groups. The microareas would bring ionic interactions that would provide a more important surface reticulation. The experimental results showed that after 30 days the surface energy was higher for the mixture plasma than for the allylamine or acrylic acid plasmas. Then the mixture would lead to a more reticulated film, and the existence of microareas is quite possible.

Finally, for the mixture plasma, we proposed a polymerization mechanism with NH_3^+/CO_2^- microareas that could bring an important surface reticulation because of ionic interactions. This treatment yielded characteristics similar to these observed for PS (adherence percentage, cells spreading, doubling time, and cellular survival).

Plasma polymerization with a allylamine/acrylic acid mixture permitted the optimum endothelialization of porcine aorta endothelial cells.

CONCLUSIONS

To improve endothelialization, the Silastic® surface was modified by plasma polymerization. We have clearly shown that plasmas of allylamine, acrylic acid, and allylamine/acrylic acid mixture gave good results. Higher hydrophilicity of the Silastic® surface was obtained because of the introduction of polar functional groups.

From the XPS analysis it was clear that plasma polymerization led to deposited layers that included C, O, and N species, depending on the kind of monomer. This was confirmed by FTIR–ATR and SEM. Nevertheless, experiments demonstrated that acquired wettability was not permanent. It decreased with time and stabilized after some days. The surface was not completely crosslinked, which allowed movement of macromolecular chains, with polar groups returning toward material bulk to minimize interfacial energy. But the initial characteristics of plasma treatment were regained when the sample were put into water. Because an organism is an aqueous media, we thought that plasma polymerization on the surface of materials would improve their biocompatibility. This was confirmed by biological studies. Adherence and growth studies of porcine aorta endothelial cells were performed, with results showing that Silastic® treated by allylamine or/and acrylic acid plasma was very interesting. The best results were obtained with a mixture plasma. Indeed, we obtained the same optimum cellular growth characteristics as those observed for the tissue culture polystyrene plate.

Silastic® treated by mixture plasma seems to be an exploitable process, for example, in the development of bioartificial substitutes, as hemocompatible vascular prostheses, or as artificial corneas. In the future the biocompatibility of this new surface will be evaluated by *in vitro* cellular tests using human endothelial cells (saphenous vein cells).

References

1. Encyclopedia of Polymer Science and Engineering, Wiley-Interscience: New York, 1985; Vol. 2, p 267.
2. Vam Wachen, P. B.; Vrerichs, C. M.; Beugelin, T.; Feijen, F. J Biomed Mat Res 1987, 21, 701.
3. Absolom, D. R.; Hawthorn, L. A.; Chang, G. J Biomed Mater Res 1988, 22, 271.
4. Curtis, A. S.; Forrestier, J. V.; McInnes, C.; Lawrie, F. J Cell Biol 1983, 97, 1500.
5. Ertel, S. I.; Chilikoti, A.; Horbett, T. A. J Biomed Mater Res 1990, 24, 1637.
6. Ertel, S. I.; Chilikoti, A.; Horbett, T. A.; Ratner, B. D. J Biomater Sci Polym 1991, 3, 163.
7. Peskin, E. ; Kiremitci, M.; Denkbas, E. B.; Gurhan, I. Clin Mater 1992, 11, 171.
8. Bradley, B. K.; Weisz, O. A.; Schnaar, R. L. J Biol Chem 1997, 262, 6431.
9. Klein Soyer, C.; Hemmendinger, S.; Cazenave, J. P. Biomaterials 1980, 52, 9.
10. Shen, M. Plasma Chemistry of Polymers; Marcel Dekker: New York, 1976.
11. Inagaki, N. Plasma Surface Modification and Plasma Polymerization; Technomic Publishing: Lancaster, PA, 1996
12. Fourche, G. Polym Eng Sci 1995, 35, 968.
13. Bruck, S. D. Properties of Biomaterials in the Physiological Environment; CRC Press: Boca Raton, FL, 1980.
14. Shimamoto, A.; Kanemitsu, S.; Fujinaga, K.; Takao, M.; Onoda, K.; Shimono, T.; Tanaka, K.; Shimpo, H.; Yada, I. Ann Thorac Surg 2000, 69, 115.
15. Lee, S. D.; Hsiue, G. H.; Kao, C. Y.; Chang, P. C. T. Biomaterials 1996, 17, 587.
16. Everaert, E. P. J. M.; Van de Belt-Gritter, B.; Van der Mei, H. C.; Busscher, H. J.; Verkerke, G. J.; Dijk, F.; Mahieu, H. F.; Reitsmer, A. J Mater Sci: Mater Med 1998, 9, 147.
17. (a) Gaboury, S. R.; Urban, M. W. Langmuir 1993, 9, 3225; (b) Gaboury, S. R.; Urban, M. W. Langmuir 1994, 10, 2289.
18. Schonherr, H.; Van Os, M. T.; Forch, R.; Timmons, R. B.; Knoll, W.; Vancso, G. J Chem Mater 2000, 12, 3689.
19. Gobotz, W. R.; Hoffman, A. S. J Appl Polym Sci, Appl Polym Symp 1988, 42, 285.
20. Mas, A.; Jaaba, H.; Schué, F.; Belu, A. M.; Cassis, C.; Linton, R. W.; Desimone, J. M. Macromol Chem Phys 1996, 197, 2331.
21. Beamson, G.; Briggs, D. High Resolution XPS of Organic Polymers, The Scienta ESCA 300 Database; Wiley: New York, 1992.
22. Briggs, D.; Seah, M. P. Practical Surface Analysis, 2nd ed.; Wiley: Chichester, England, 1990; Vol. 1.
23. Mazzucotelli, J. P.; Lecouls, L.; Hamzaoui, A.; Philippon, C. ; Bizouard, E.; Moczar, M.; Loisance, D. Artif Organs 1996, 20(1), 30.
24. Murakami, T.; Kuroda, S.; Osawa, Z. J Colloid Interface Sci 1998, 202, 37.
25. Paynter, R. W. Surf. Interface Anal 1999, 27, 103.
26. Dupond-Gillain, C. C.; Adriaensen, Y.; Derclaye, S.; Rouxhet, P. G. Langmuir 2000, 16, 8194.
27. Morra, M.; Occhiello, E.; Garbassi, F. J Colloid Interface Sci 1992, 149, 84.
28. Bell, A. T.; Wydeven, T.; Johnson, C. C. J Appl Polym Sci 1975, 19, 1911.
29. Inagaki, N.; Tasaka, S.; Yamada, Y. J Polym Sci, Part A: Polym Chem 1992, 30, 2003.
30. Mas, A.; Jaaba, H.; Schué, F.; Belu, A. M.; Cassis, C.; Linton, R. W.; Desimone, J. M. Makromo Chem Phys 1997, 198, 3737.
31. Bruil, A.; Terlingen, J. G. A.; Beugeling, T.; Van Aken, W. G.; Feijen, J. Biomaterials 1995, 13, 915.